



CHORUS

This is the accepted manuscript made available via CHORUS. The article has been published as:

Adiabatic Cooling of Antiprotons

G. Gabrielse, W. S. Kolthammer, R. McConnell, P. Richerme, R. Kalra, E. Novitski, D. Grzonka, W. Oelert, T. Sefzick, M. Zielinski, D. Fitzakerley, M. C. George, E. A. Hessels, C. H. Storry, M. Weel, A. Müllers, and J. Walz (ATRAP Collaboration)

Phys. Rev. Lett. **106**, 073002 — Published 15 February 2011

DOI: [10.1103/PhysRevLett.106.073002](https://doi.org/10.1103/PhysRevLett.106.073002)

Adiabatic Cooling of Antiprotons

G. Gabrielse,* W.S. Kolthammer, R. McConnell, P. Richerme, R. Kalra, and E. Novitski
Dept. of Physics, Harvard University, Cambridge, MA 02138

D. Grzonka, W. Oelert, T. Sefzick, and M. Zielinski
IKP, Forschungszentrum Jülich GmbH, 52425 Jülich, Germany

D. Fitzakerley, M.C. George, E.A. Hessels, C.H. Storry, and M. Weel
York University, Department of Physics and Astronomy, Toronto, Ontario M3J 1P3, Canada

A. Müllers and J. Walz
Institut für Physik, Johannes Gutenberg Universität and Helmholtz Institut Mainz, D-55099 Mainz, Germany
 (ATRAP Collaboration)

Adiabatic cooling is shown to be a simple and effective method to cool many charged particles in a trap to very low temperatures. Up to 3×10^6 \bar{p} are cooled to 3.5 K. This is 10^3 time more cold \bar{p} and a 3 times lower \bar{p} temperature than previously reported. A second cooling method cools \bar{p} plasmas via the synchrotron radiation of embedded e^- (with many fewer e^- than \bar{p}) in preparation for adiabatic cooling. No \bar{p} are lost during either process – a significant advantage for rare particles.

Much energy and effort is required to produce modest numbers of antiprotons (\bar{p}) – the stable antimatter nucleon. Reducing \bar{p} energy to form cold antihydrogen (\bar{H}) atoms is a big additional challenge. Years of effort have gone towards realizing the original proposal [1] to capture cold \bar{H} atoms in magnetic traps for precise spectroscopy and tests of fundamental symmetries. The latest significant step is an atom confined for a small fraction of a second in 1 of 9 trials [2]. However, greatly improved \bar{p} cooling methods are needed to attain usable numbers of trapped \bar{H} for useful times in known excitation states, and to increase low energy \bar{p} beam luminosity.

Two new cooling methods reported in this Letter together produce the largest cold \bar{p} plasmas – 3×10^6 \bar{p} at 3.5 ± 0.7 K. For comparison, evaporative cooling recently reported in this journal [3], yielded 10^3 times fewer trapped \bar{p} at nearly 3 times the temperature. The central demonstration here is of adiabatic cooling. Also crucial is the embedded e^- cooling that prepares the \bar{p} for adiabatic cooling. Many fewer e^- than \bar{p} are used, just the opposite of the e^- cooling method [4] used to obtain all cold \bar{p} and \bar{H} atoms so far. The number of e^- present during both types of cooling, many fewer than the e^+ used to form \bar{H} , should be small enough to not inhibit \bar{H} production. Even lower \bar{p} temperatures should be possible with embedded e^- cooling, followed by adiabatic cooling, followed by evaporative cooling.

Adiabatic cooling in a harmonic trap potential takes place when the restoring force F and potential energy well U are reduced while these confine a plasma initially at temperature T_i . A measure of F and U is the oscillation frequency f of the plasma's center-of-mass in the well, since $\omega = 2\pi f$ determines $F = -m\omega^2 z$ and

$U = m\omega^2 z^2/2$. Adiabatic cooling takes T_i to T_f as f_i is reduced to f_f .

For a low particle density, adiabatic cooling of \bar{p} oscillators [5], implications for the energy analysis of the first trapped [6] and electron-cooled [4] \bar{p} , and cooling of hot ions for FTICR [7] have been considered. A particle oscillator's energy E decreases as its oscillation frequency f is reduced adiabatically because E/f is a familiar adiabatic invariant – the invariant quantized in quantum mechanics. The prediction is thus $T_f = (f_f/f_i) T_i$. If a coupled oscillatory motion contributes heat capacity but no additional cooling (e.g. \bar{p} cyclotron motion) then the individual particle prediction is $T_f = (f_f/f_i)^{1/2} T_i$.

The density of the plasmas for this demonstration is high enough to make the Debye length smaller than the plasma size. The plasmas are weakly correlated, with a kinetic energy larger than the Coulomb repulsion energy between neighboring \bar{p} , on average. The \bar{p} within the plasma thus move and collide within the plasma boundary approximately as an ideal gas (viewed in the appropriate rotating reference frame [8]). The prediction for an ideal gas [8, 9] is

$$T_f = (V_i/V_f)^{2/3} T_i. \quad (1)$$

Adiabatic cooling takes place when the restoring force does negative work on the plasma to increase its volume V and decrease its temperature T , all with no entropy change.

The adiabatic condition for low \bar{p} density is that f changes very little during an oscillation period, $\dot{f}/f \ll f$. For a dense \bar{p} plasma, a plasma has been changed adiabatically and reversibly if its final temperature T_f is independent of the rate at which f is changed. For all densities, the adiabatic cooling and the measurement of T_f must take place before any other process changes the plasma temperature (e.g. embedded e^- cooling).

* Spokesperson: gabrielse@physics.harvard.edu

The $N_p = 2 \times 10^5$ to 3×10^6 \bar{p} used for the trials reported here are accumulated from 1 to 21 injection pulses of \bar{p} from CERN's unique Antiproton Decelerator. The trapping [6], electron-cooling [4] and stacking [10] methods that have accumulated up to 1.1×10^7 \bar{p} at ATRAP are those employed for all \bar{H} experiments [11]. The \bar{p} slow within a thin degrader window, are captured in a trap formed by biasing electrodes that surround the \bar{p} , and cool via collisions with a large number of surrounding e^- . Typically $N_e = 10^8$ photoelectrons are used after they are liberated from a metal surface by intense ultraviolet pulses from an excimer laser [12]. A ‘‘rotating wall’’ drive [13] compresses a spheroidal e^- plasma to a 2 mm radius, and the plasma cools via e^- synchrotron radiation. After \bar{p} are loaded they cool via collisions with the cold e^- . Centrifugal forces on the simultaneously rotating \bar{p} and e^- plasmas separate them radially [14] so the \bar{p} are farther from the trap axis.

Directly manipulating trapped \bar{p} , measuring their temperature, and using them for experiments is difficult if $N_e \gg N_p$, as in standard e^- cooling. \bar{H} production, for example, would be inhibited if e^- substitute for e^+ in what would otherwise be the replacement collisions [15] that form more deeply bound \bar{H} atoms. The inverted situation for embedded e^- cooling, with $N_p \gg N_e$ and each e^- surrounded by many \bar{p} , cools \bar{p} much more slowly but no less effectively. To investigate embedded e^- cooling, most of the e^- are ejected along the trap's center axis using a method introduced along with e^- cooling [4]. The depth of the trap containing the \bar{p} and e^- is pulsed to 0 eV. The pulses are long enough that e^- thermal velocities can take them out of the well before the well is restored, but short enough that the heavier \bar{p} cannot escape. Three or four pulses leave all of the \bar{p} in the trap, along with $N_e = 6 \times 10^3$ or 9×10^2 e^- (estimated from observed heating rates below). After the ejection raises the \bar{p} temperature to typically hundreds of K, embedded e^- cooling cools the \bar{p} by an order of magnitude in temperature.

The \bar{p} and remaining e^- are confined in a potential well made by biasing gold-plated, copper ring electrodes (Fig. 1a) with a $B = 3.7$ T field along their symmetry axis. The electrodes shown are part of a stack of 39 electrodes (represented fully in [16]). The potential applied to electrode LTE2 in Fig. 1a determines the empty-trap well depth W_0 (eg. Figs. 1b-c), and also the small-amplitude oscillation frequency f for a single \bar{p} in the otherwise empty well. (Thus f characterizes an empty well rather than being defined as an oscillation frequency of a trapped plasma.) Plasma space charge reduces the energy required for a \bar{p} to escape the plasma and trap (along the z -axis) to $W \leq W_0$ (Fig. 1c). The dependence of W on W_0 and f , along with N_p and plasma geometry, is calculated with finite difference methods [17].

The small number of e^- embedded within the \bar{p} cool or heat the plasma to a temperature T_i . This steady-state T_i is determined by blackbody radiation from the trap electrodes and by electrical noise that drives the parti-

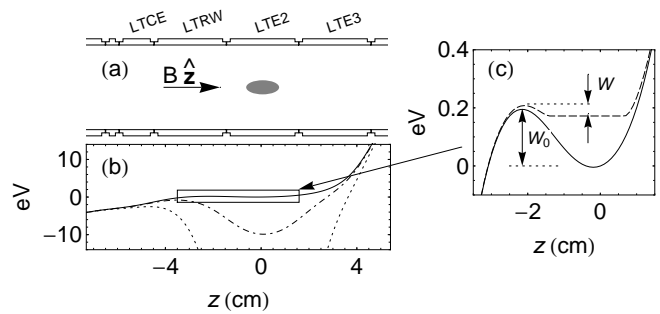


FIG. 1. (a) Cross section of trap electrodes with the location of the \bar{p} plasma. (b) On-axis potential energies for \bar{p} on the trap axis for W_0 of 0.2, 9 and 77 eV. (c) Expanded view without (solid curve) and with (dashed curve) the space charge potential energy for $N_p = 5 \times 10^5$.

cles directly. The time scale for embedded e^- cooling is that required to cool N_p antiprotons via the synchrotron radiation of N_e electrons, each at a rate $\gamma_c = 4r_0\omega_c^2/3c = (0.2 \text{ s})^{-1}$. (Here r_0 is the classical electron radius, ω_c is the e^- cyclotron frequency, and c is the speed of light.) On average, a \bar{p} in the plasma thus cools at the rate $\gamma_p = \gamma_c N_e/N_p$. The assumption that the energy of the \bar{p} is transferred to the e^- via collisions at a rate $\gamma_{ep} \gg \gamma_p$, justified below, is possible since $(\gamma_p)^{-1} \geq 17$ s for our trials. The coupled rate equations that describe the \bar{p} and e^- temperatures [5] simplify to equal \bar{p} and e^- temperatures, T , with $dT/dt = -\gamma_p(T - T_i)$. For times $t \gg (\gamma_p)^{-1}$, the \bar{p} and e^- share the steady-state temperature, T_i . Adiabatic cooling to $T < T_i$ is observed if cooling is complete and T measured in time $t \ll (\gamma_p)^{-1}$.

Collision rates within the plasma are fast compared to γ_p . For $B = 0$, a classic treatment [18] gives a \bar{p} - e^- collision rate 10^6 times larger than γ_p for our plasmas. The rate for collisions that couple radial and axial energy is suppressed when a strong B is added along the trap axis [19]. Even with the predicted suppression by a factor of 10^3 , the axial-radial collision rate is much faster than γ_p , with a time constant shorter than 0.01 s for even our lowest temperatures. Since the biggest effect of B is to inhibit the axial-radial coupling, we assume that the \bar{p} - e^- collision rate γ_{ep} is also larger than γ_p by at least 3 orders of magnitude.

Adiabatic cooling starts with an initial f_i chosen to be between 3 MHz and 90 kHz, corresponding to W_0 between 800 and 0.4 eV on axis. The initial f_i is lowered to f_f , the latter corresponding to a well depth W just big enough to keep \bar{p} from escaping. The adiabatic cooling is completed in hundreds of ms, with the cooling result the same when this time is varied by a factor of 5. The cooling time is short compared to $(\gamma_p)^{-1}$, so that embedded e^- cooling has negligible effect during adiabatic cooling.

The \bar{p} plasma temperature after adiabatic cooling is revealed [20] by the first few thousand \bar{p} that escape (too few to modify T) as W_0 is reduced linearly at 2.2 eV/s to the value at which \bar{p} escape, at a W_0 that corresponds to f_f . Thermal energy allows the initial \bar{p} to escape over the

potential barrier, along \hat{z} to the left in Figs. 1b-c. Over the range of the plasma temperatures in this report, f_f (determined mostly by space charge) varies by $\pm 2\%$. The number escaping, dN_p , for a series of small reductions in the empty trap well depth, dW_0 , is counted as a function of W_0 . Surrounding scintillators detect \bar{p} annihilations with a 75% efficiency. Each \bar{p} loss spectrum in Fig. 2a shows the first antiprotons escaping as a sharp edge to the right (expanded examples in Fig. 2b). The edges are at larger W_0 for larger N_p . Variations of about 10 meV, from variations in N_p and the plasma radius, are small and do not change the slope of the edges. For a Boltzmann distribution, $\ln(dN_p/dW) \propto -W/kT$. The conversion between W and W_0 used to convert the measured dN_p/dW_0 comes from the finite difference calculations. If space charge is neglected (i.e. $W = W_0$ assumed), the incorrectly deduced T for $N_p = 5 \times 10^5$ would typically be 1.3 to 2 times larger, the latter for the lowest temperatures.

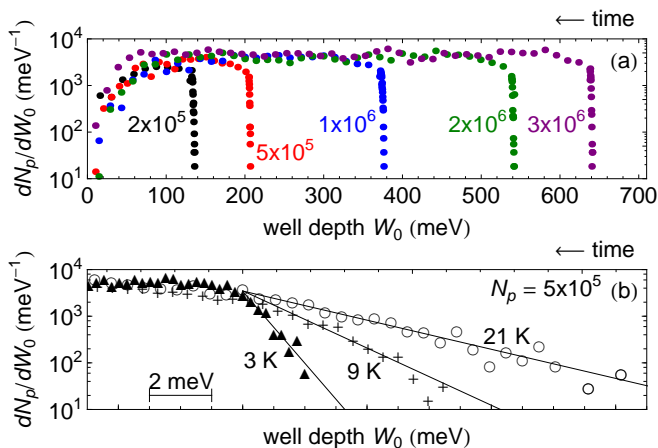


FIG. 2. (a) Superposition of \bar{p} loss spectra for indicated N_p as W_0 is reduced linearly in time (i.e. right to left). (b) T is determined from the exponential slope of the first thousand \bar{p} to escape as W_0 is reduced. The three examples are aligned so the slopes can be readily compared.

Adiabatic cooling produces the lowest \bar{p} temperatures directly measured, $T = 3.5 \pm 0.7$ K (the gray band of Fig. 3 for $f_i > 400$ kHz). Before leveling off at this value, the measured T fits to a power law in f_i for the well within which embedded e^- establish initial equilibrium at $T_i = 31$ K. (A noise drive applied to a nearby electrode increases T_i to this easily observed value from what otherwise would be 17 K.) The frequency f_f describes the well from which \bar{p} begin to escape. The uncertainties on the points indicate measurement reproducibility.

What prevents observed temperatures that are even lower is not yet understood. One possibility is that the lowest measured T (the same for all N_p , T_i , and $f_i > 400$ kHz utilized) is a measurement limit for the apparatus and method. The actual \bar{p} temperatures could then be much lower, as low as 0.4 K if the best fit power law is extrapolated to the largest f_i used. However, no physical

cause for such a limit has yet been identified. A second possibility is that some technical noise keeps the \bar{p} from reaching a lower T , but the source of such noise has not yet been found. A third possibility is that the better theoretical understanding needed for adiabatic cooling will reveal a slope change at $f_i \approx 400$ kHz in Fig. 3.

The cooling in Fig. 3 is more effective than predicted for small f_f/f_i . The ideal gas prediction uses Eq. 1 with plasma volumes from the finite difference calculations for realistic trap potentials. The prediction does not change noticeably when the volumes are approximated as spheroids [21] (the required plasma shape within an electrostatic quadrupole potential). Of course, the \bar{p} plasma is not an ideal gas of constant density within sharply defined boundaries. The density actually drops off over a temperature-dependent Debye length that has yet to be included in the theoretical description. Also compared in Fig. 3 are predictions $T \propto f_i^{-1}$ and $T \propto f_i^{-1/2}$ from the familiar adiabatic invariant of an oscillator.

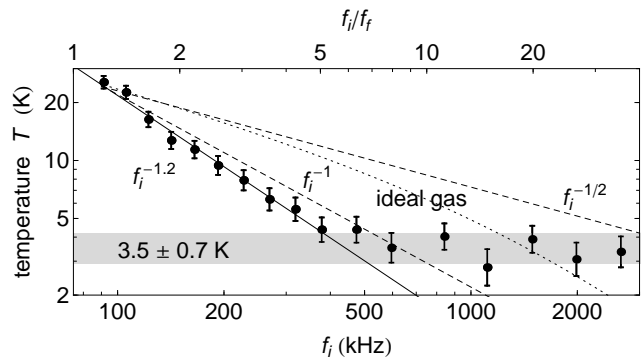


FIG. 3. Measured and predicted temperatures for 5×10^5 \bar{p} after adiabatic cooling. The measured T fits a power law (solid curve) down to the lowest T measured (gray band).

An important feature of adiabatic cooling is that no particle loss is expected or observed. This makes it possible to cool large numbers of \bar{p} . This is important for low energy \bar{p} experiments given that \bar{p} are not readily available. For example, the long term goal of trapping \bar{H} atoms for precise laser spectroscopic comparisons to hydrogen atoms [1] requires as many cold atoms with energies below 0.5 K as possible. This energy is the depth of the deepest magnetic traps for \bar{H} atoms that can be constructed with state-of-the-art superconducting technology. Larger numbers of colder \bar{p} would seem to be a necessary (though not sufficient) step towards useful numbers of trapped \bar{H} atoms.

Figure 4 illustrates the slow return to equilibrium at T_i after adiabatic cooling. The rate γ_p is faster with more e^- (after 3 rather than 4 ejection pulses). An exponential fit determines N_e in terms of the separately measured N_p since $\gamma_p = \gamma_c N_e/N_p$. Both curves in Fig. 4 rise to the same T_i , suggesting that e^- rather than \bar{p} are being heated to make $T_i > 1.2$ K (the electrode temperature [22]). A consistent γ_p can be similarly and independently determined from the T measured as \bar{p} cool to T_i .

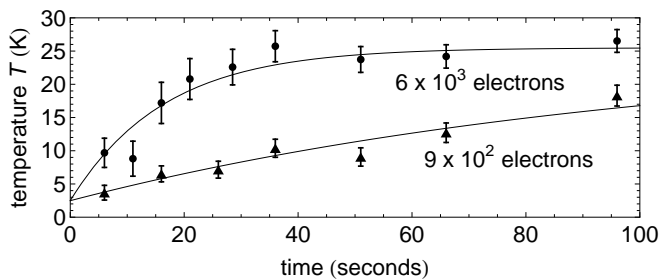


FIG. 4. After adiabatic cooling of $5 \times 10^5 \bar{p}$, thermal equilibrium at T_i is slowly reestablished at a rate γ_p that increases with N_e . The $T = 2.5$ K at the left is consistent with best-fit of the measured T in Fig. 3.

The embedded e^- cooling of \bar{p} that establishes $T_i = 17$ K is also important on its own, e.g. to remove heat added when particles are moved to new locations. Reducing noise that heats the e^- (perhaps from radio or TV stations, or from the many electrical signals in the decelerator hall) should make T_i approach the 1.2 K electrode temperature, and an even lower T after subsequent adiabatic cooling.

Finally, adiabatic cooling is naturally compatible with

producing \bar{H} that can be trapped insofar as the \bar{p} rotation velocities are low in the shallow well at the conclusion of the cooling. \bar{H} formed with such velocities could be captured a magnetic trap.

In conclusion, adiabatic cooling is shown to be an effective method for cooling far more \bar{p} than have previously been cooled. The \bar{p} are cooled to $T = 3.5 \pm 0.7$, the lowest directly measured \bar{p} temperature. Adiabatic cooling thus promises to be an important method for attain usable numbers of \bar{H} atoms that are cold enough to be confined in a magnetic trap. The \bar{p} are prepared for adiabatic cooling using embedded electron cooling. This cooling method, shown to cool many \bar{p} with much fewer e^- , has some promise on its own. Orders of magnitude more cold \bar{p} are produced by embedded electron cooling followed by adiabatic cooling than by evaporative cooling, in part because the latter requires significant particle loss. Embedded electron cooling, followed by adiabatic cooling, followed by evaporative cooling should give much lower \bar{p} temperatures.

We are grateful to CERN for the 5-MeV \bar{p} from its Antiproton Decelerator. This work was supported by the NSF and AFOSR of the US, the BMBF, DFG, and DAAD of Germany, and the NSERC, CRC, CFI and ERA of Canada. W.O. is supported in part by CERN.

-
- [1] G. Gabrielse, in *Fundamental Symmetries*, edited by P. Bloch, P. Pavlopoulos, and R. Klapisch (Plenum, New York, 1987) pp. 59–75.
- [2] G. B. Andresen and *et al.* (ALPHA Collaboration) doi:10.1038/nature09610 (in press).
- [3] Andresen, G. B. *et al.* (ALPHA Collaboration), *Phys. Rev. Lett.* **105**, 013003 (2010).
- [4] G. Gabrielse, X. Fei, L. A. Orozco, R. L. Tjoelker, J. Haas, H. Kalinowsky, T. A. Trainor, and W. Kells, *Phys. Rev. Lett.* **63**, 1360 (1989).
- [5] S. L. Rolston and G. Gabrielse, *Hyperfine Interact.* **44**, 233 (1988).
- [6] G. Gabrielse, X. Fei, K. Helmerson, S. L. Rolston, R. L. Tjoelker, T. A. Trainor, H. Kalinowsky, J. Haas, and W. Kells, *Phys. Rev. Lett.* **57**, 2504 (1986).
- [7] M. V. Gorshkov, C. D. Masselon, G. A. A. H. R. Udseth, R. Harkewicz, and R. D. Smith, *Journal of the American Society for Mass Spectrometry* **12**, 1169 (2001), ISSN 1044-0305.
- [8] T. M. O’Neil and D. H. E. Dubin, *Phys. Plas.* **5**, 2163 (1998).
- [9] G. Z. Li, R. Poggiani, G. Testera, and G. Werth, *Hyperfine Interact.* **76**, 281 (1993).
- [10] G. Gabrielse, N. S. Bowden, P. Oxley, A. Speck, C. H. Storry, J. N. Tan, M. Wessels, D. Grzonka, W. Oelert, G. Schepers, T. Seifick, J. Walz, H. Pittner, and E. A. Hessels, *Phys. Lett. B* **548**, 140 (2002).
- [11] G. Gabrielse, *Adv. At. Mol. Opt. Phys.* **45**, 1 (2001).
- [12] B. Levitt, G. Gabrielse, P. Larochele, D. Le Sage, W. S. Kolthammer, R. McConnell, J. Wrubel, A. Speck, D. Grzonka, W. Oelert, T. Seifick, Z. Zhang, D. Comeau, M. C. George, E. A. Hessels, C. H. Storry, M. Weel, and J. Walz, *Phys. Lett. B* **656**, 25 (2007).
- [13] X. P. Huang, F. Anderegg, E. M. Hollmann, C. F. Driscoll, and T. M. O’Neil, *Phys. Rev. Lett.* **78**, 875 (1997).
- [14] G. Gabrielse, W. S. Kolthammer, R. McConnell, P. Richerme, J. Wrubel, R. Kalra, E. Novitski, D. Grzonka, W. Oelert, T. Seifick, M. Zielinski, J. S. Borbely, D. Fitzakerley, M. C. George, E. A. Hessels, C. H. Storry, M. Weel, A. Müllers, J. Walz, and A. Speck, *Phys. Rev. Lett.* **105**, 213002 (2010).
- [15] M. Glinzky and T. O’Neil, *Phys. Fluids* **B3**, 1279 (1991).
- [16] G. Gabrielse, P. Larochele, D. Le Sage, B. Levitt, W. S. Kolthammer, R. McConnell, P. Richerme, J. Wrubel, A. Speck, M. C. George, D. Grzonka, W. Oelert, T. Seifick, Z. Zhang, A. Carew, D. Comeau, E. A. Hessels, C. H. Storry, M. Weel, and J. Walz, *Phys. Rev. Lett.* **100**, 113001 (2008).
- [17] R. L. Spencer, S. N. Rasband, and R. R. Vanfleet, *Phys. Fluids B* **5**, 4267 (1993).
- [18] L. Spitzer, Jr., *Physics of Fully Ionized Gases* (Dover, 1962).
- [19] M. E. Glinzky, T. M. O’Neil, M. N. Rosenbluth, K. Tsunura, and S. Ichimaru, *Phys. Fluids* **4**, 1156 (1992).
- [20] D. L. Eggleston, C. F. Driscoll, B. R. Beck, A. W. Hyatt, and J. H. Malmberg, *Phys. Fluids B* **4**, 3432 (1992).
- [21] G. Z. Li, R. Poggiani, G. Testera, and G. Werth, *Z. Phys. D* **22**, 375 (1991).
- [22] J. Wrubel, *et al.* (ATRAP Collaboration), (to be published).